Influence of elastic element parameters on stress distribution and reaction forces in shaft support systems of sawing cylinders

Shakhnoza Makhmudova[1], Gulnora Yuldasheva[2], Feruza Azimova[3], Dilafruz Akhmedova[4]
[1, 2, 4]Department of Materials Science and Mechanical Engineering, Tashkent State Transport University, Tashkent, Uzbekistan
[3]Department of Industrial Economy, Tashkent State Transport University, Tashkent, Uzbekistan
[1]Corresponding author
E-mail: [1]*maxmudovash88@gmail.com*, [2]*yuldashevagulnora123@gmail.com*, [3]*fiyruza2405@icloud.com*, [4]*d.akhmedova@mail.ru*

Received 18 March 2026; accepted 7 April 2026; published online 8 June 2026
DOI https://doi.org/10.21595/vp.2026.26416

76th International Conference on Vibroengineering in Tashkent, Uzbekistan, April 28-29, 2026

Abstract. This study investigates the effect of elastic element thickness variation in combined shaft supports on stress distribution and reaction forces in sawing cylinder systems. Two computational models were developed: (1) with elastic element thickness at support A greater than or equal to support B ($A \geq B$), and (2) with thickness at support B greater than or equal to support A ($B \geq A$). The analysis demonstrates that variations in elastic element thickness significantly influence stress distribution and reaction forces in the system. When the thickness at support A exceeds that at support B, shaft stresses decrease from 198×10^6 to 112×10^6 Pa, while reaction force at support B decreases from 943.24 N to 918.02 N. Conversely, when the thickness at support B exceeds that at support A, stresses increase from 8.83×10^6 to 183×10^6 Pa, with reaction force at B increasing from 899.04 N to 931.19 N. The results show that optimizing elastic element parameters can significantly reduce operational stresses in shaft support systems.

Keywords: elastic support, shaft dynamics, stress analysis, reaction forces, sawing cylinder, finite element analysis, mechanical design.

1. Introduction

Rotating shaft systems represent fundamental components of many industrial machines, including textile equipment, woodworking machinery, and precision cutting mechanisms. The operational reliability of such systems strongly depends on the design of the supporting structures, which must ensure both accurate positioning of the shaft and effective transmission of loads during operation. Improper support design often leads to uneven load distribution, increased vibration levels, and premature failure of mechanical components [1]-[3].

Sawing cylinders used in cotton-processing and woodworking machines are typical examples of rotating elements subjected to complex loading conditions. During operation, the shaft experiences combined effects of static forces, dynamic loads, and periodic disturbances generated by cutting interactions. These conditions create significant stresses within the shaft and its supporting elements, which may reduce service life and lead to structural damage if not properly controlled [4], [5].

Traditional shaft support systems frequently employ rigid bearing housings. Although such configurations provide high structural stiffness, they often lack the ability to accommodate dynamic load variations and misalignment effects. As a result, stress concentrations may occur in critical sections of the shaft, especially in high-speed rotating machinery [6], [7]. In recent years, the integration of elastic elements into support structures has been proposed as an effective approach to improving load distribution and reducing vibration amplitudes in rotor systems [8], [9].

Elastic supports introduce additional compliance into the mechanical system, allowing partial redistribution of loads between support points and reducing stress peaks within the shaft. Furthermore, elastic elements may contribute to vibration damping and improved dynamic stability of rotating machinery [10], [11]. The mechanical behaviour of such systems, however, depends strongly on the stiffness characteristics and geometric parameters of the elastic elements used in the support structure.

A considerable number of studies have been devoted to the dynamic analysis of rotor-bearing systems. Classical rotordynamic theories developed by Nelson, Childs, and other researchers established the fundamental principles of rotor stability and vibration behaviour [12]-[14]. Later studies applied finite element modelling techniques to analyse the dynamic response of flexible shafts supported by different types of bearings and support structures [15]-[17]. These approaches have significantly improved the understanding of rotor dynamics and vibration control in modern machinery.

Despite these advances, the specific influence of elastic element geometry on stress distribution in shaft support systems remains insufficiently explored. In many engineering applications, the stiffness of elastic elements is determined primarily by their material properties and thickness. Variations in thickness may therefore alter the load distribution between supports and significantly influence the stress state of the shaft [18], [19]. However, quantitative relationships between elastic element thickness and resulting reaction forces are rarely discussed in existing literature.

Therefore, the present study investigates the influence of elastic element thickness in combined shaft supports on the stress distribution and reaction forces in a sawing cylinder system. Two support configurations are considered, differing in the relative thickness of elastic elements at the support points. The analysis aims to determine how variations in these geometric parameters affect the mechanical response of the shaft system and to identify configurations that minimize operational stresses.

The results of this research provide practical recommendations for optimizing elastic support parameters in rotating machinery. Such optimization can contribute to improved durability, reduced vibration levels, and increased operational reliability of sawing cylinder mechanisms and similar shaft systems.

Recent studies have proposed analytical models of rotor-bearing-housing systems that take into account additional elastic-dissipative layers within the support structure [21]. Such approaches allow evaluating the influence of polymer inserts on resonance frequencies and vibration characteristics of rotating systems.

The novelty of this study lies in the following aspects:

– Investigation of asymmetric elastic element thickness in combined shaft support systems.

– Establishment of quantitative relationships between elastic element geometry and stress distribution.

– Analysis of reaction force redistribution depending on support stiffness variation.

– Identification of optimal thickness configuration for minimizing stresses in sawing cylinder shaft systems.

2. Materials and methods

This study presents a numerical investigation of the stress-strain state and load distribution in a sawing cylinder shaft system with elastic support elements. The analysis was carried out using the finite element method (FEM) to evaluate the influence of elastic element thickness on reaction forces and stress distribution.

2.1. Geometrical model

The developed three-dimensional model of the sawing cylinder shaft system, including the

shaft, rolling bearings, and elastic support elements, is illustrated in Fig. 1.

The shaft is modeled as a homogeneous cylindrical element with a total length of 2300 mm, supported at two points (supports A and B). The bearing outer diameter is taken as 100 mm, corresponding to typical industrial configurations.

The shaft is supported by rolling bearings mounted in housings. Elastic elements are introduced between the bearing housings and the machine frame to simulate flexible support conditions.

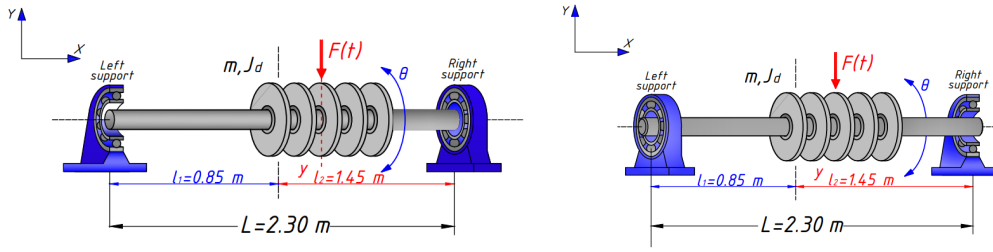

a) Load case $A > B$ b) Load case $B > A$

Fig. 1. Three-dimensional model of the sawing cylinder shaft system with elastic support elements.

2.2. Material properties

The shaft material was assumed to be isotropic and linearly elastic. The following mechanical properties were used in the simulation:

– Young's modulus: $E = 2.1 \times 10^{11}$ Pa.

– Poisson's ratio: $\nu = 0.3$.

– Density: $\rho = 7850$ kg/m^3.

The elastic support elements were modeled as deformable layers with reduced stiffness. Their mechanical behavior was characterized by an equivalent elastic modulus corresponding to polymer-based materials.

2.3. Finite element model

The numerical analysis was performed using the finite element method (FEM). The computational model was developed using APM FEM software, while MATLAB was employed for post-processing, data analysis, and graphical visualization of the results.

The shaft was discretized using three-dimensional solid elements. A sufficiently refined mesh was applied in regions of expected stress concentration near the supports to improve the accuracy of stress evaluation.

The bearing supports were modeled as elastic constraints, allowing partial displacement depending on the stiffness of the elastic elements. The solution was obtained under static loading conditions.

2.4. Boundary conditions and loading

The shaft was subjected to operational loading conditions representing working regimes of sawing cylinders. The following assumptions were applied:

– The shaft ends were constrained in accordance with bearing support conditions.

– Radial loads were applied to simulate operational forces.

– Elastic supports were modeled as distributed compliance elements.

Two configurations of elastic element thickness were considered:

– Model 1 ($A \geq B$): thickness at support A is greater than or equal to that at support B.

– Model 2 ($B \geq A$): thickness at support B is greater than or equal to that at support A.

The thickness of elastic elements varied in the range of 0 to 1.5 mm.

2.5. Simulation parameters

For each configuration, the following parameters were calculated:
– Reaction forces at supports A and B.
– Equivalent (von Mises) stress distribution.
– Total and elastic deformations.

The results were obtained for multiple geometric configurations to identify trends in load redistribution and stress variation.

The numerical results were processed and presented in the form of tables and graphical dependencies. The relationships between elastic element thickness and system response parameters were analyzed to determine optimal configurations minimizing stress levels. This modeling approach ensures adequate accuracy for evaluating stress distribution and load transfer in shaft support systems.

3. Results and discussion

3.1. Reaction force analysis

The calculated reaction forces at the shaft supports for the configuration $A \geq B$ are summarized in Table 1. The results show that increasing the thickness of the elastic element at support A leads to a gradual redistribution of loads between the supports.

Table 1. Reaction forces for configuration $A \geq B$

No.	A (mm)	B (mm)	R_α (N)	R_β (N)
1	0	0	1188.2	902.29
2	0.50	0.25	1167.8	943.24
3	0.75	0.50	1147.4	936.21
4	1.00	0.75	1152.6	929.90
5	1.25	1.00	1158.2	923.89
6	1.50	1.25	1163.8	918.02

For comparison, the reaction forces obtained for the opposite configuration $B \geq A$ are presented in Table 2. In this case, an increase in the thickness of the elastic element at support B results in a noticeable change in the load distribution between the supports.

Table 2. Reaction forces for configuration $B \geq A$

No.	A (mm)	B (mm)	R_α (N)	R_β (N)
1	0	0	1188.2	902.29
2	0.25	0.50	1190.2	899.04
3	0.50	0.75	1175.0	913.79
4	0.75	1.00	1168.8	919.59
5	1.00	1.25	1162.6	925.39
6	1.25	1.50	1156.4	931.19

The influence of elastic element thickness on the reaction forces at the shaft supports is illustrated in Fig. 2. The graphical dependencies clearly demonstrate the redistribution of loads between supports A and B as the thickness of the elastic element varies.

The analysis reveals inverse relationships between elastic element thickness distribution and reaction forces. In Model 1 ($A \geq B$), increasing thickness at support A while maintaining $A \geq B$ ratio results in gradual reduction of R_β from 943.24 N to 918.02 N (Fig. 2(a)). Conversely, Model 2 ($B \geq A$) demonstrates increase in R_β from 899.04 N to 931.19 N as thickness at B increases

(Fig. 2(b)).

These dependencies indicate that elastic element parameters indicate a strong correlation between elastic element thickness distribution and reaction forces, enabling predictive control of support reactions through geometric optimization.

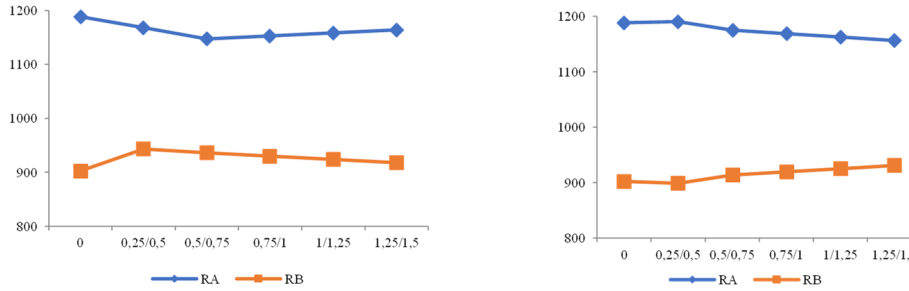

a) When $A \geq B$ b) When $B \geq A$

Fig. 2. Reaction forces at the sawing cylinder shaft supports as a function of elastic element thickness

3.2. Stress analysis

The calculated stress characteristics of the shaft for the configuration $A \geq B$ are presented in Table 3. The results indicate that increasing the thickness of the elastic element at support A leads to a gradual decrease in the average stress level within the system.

Table 3. Stress characteristics for configuration $A \geq B$

No.	A (mm)	B (mm)	σ_{min} (×10⁶ Pa)	σ_{max} (×10⁶ Pa)	σ_{avg} (×10⁶ Pa)
1	0.50	0.25	0.000205	562	198
2	0.75	0.50	0.000973	465	166
3	1.00	0.75	0.000980	364	153
4	1.25	1.00	0.001053	278	139
5	1.50	1.25	0.001090	205	112

For the alternative configuration $B \geq A$, the corresponding stress parameters are given in Table 4. In contrast to the previous case, increasing the thickness of the elastic element at support B leads to a significant growth in the stress level.

Table 4. Stress characteristics for configuration $B \geq A$

No.	A (mm)	B (mm)	σ_{min} (×10⁶ Pa)	σ_{max} (×10⁶ Pa)	σ_{avg} (×10⁶ Pa)
1	0.25	0.50	0.000802	17.7	8.83
2	0.50	0.75	0.000859	105	52.3
3	0.75	1.00	0.000916	191	95.7
4	1.00	1.25	0.000973	278	139
5	1.25	1.50	0.001030	365	183

The effect of elastic element thickness on the stress state of the system is further illustrated in Fig. 3. The graphical dependencies confirm the trends observed in the numerical results and highlight the strong influence of support stiffness distribution on shaft stresses.

Stress analysis reveals dramatic differences between configurations. Model 1 ($A \geq B$) demonstrates stress reduction from 198×10⁶ Pa to 112×10⁶ Pa as thickness differential increases (Fig. 3(a)). This 43.4 % reduction indicates significant potential for fatigue life extension.

In contrast, Model 2 ($B \geq A$) shows a significant increase in stress from 8.83×10⁶ Pa to 183×10⁶ Pa, corresponding to more than a twentyfold increase.

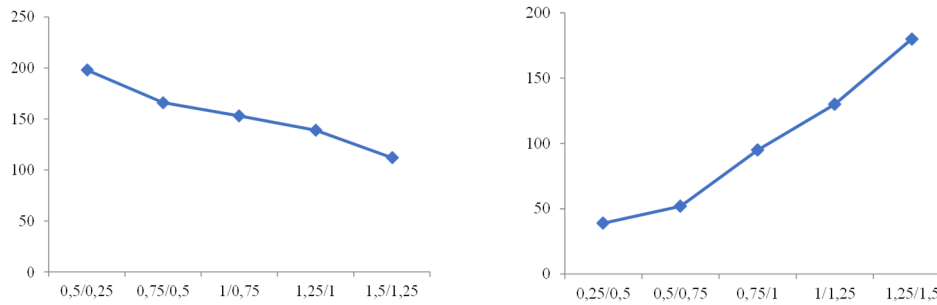

a) When $A \geq B$ b) When $B \geq A$

Fig. 3. Dependence of system stress on elastic element thickness

3.3. Deformation characteristics

Deformation analysis (Tables 3-4) reveals that minimum deformations transition from positive to negative values as thickness increases, indicating shift from tensile to compressive stress states. Maximum deformations decrease with increasing thickness in Model 1 ($1800 \rightarrow 1120 \times 10^{-6}$ m) while increasing in Model 2 ($1300 \rightarrow 1720 \times 10^{-6}$ m), confirming stress redistribution patterns.

The obtained results demonstrate that the distribution of elastic element thickness in combined shaft supports represents an important design parameter for controlling the stress state of rotating shaft systems. The inverse relationship observed between the thickness of the elastic element at support A and the stress level in the shaft (Model 1) is consistent with theoretical concepts of stiffness redistribution in rotor–bearing systems [12], [17].

The results indicate a substantial difference between the two investigated configurations. In particular, the stress level in the shaft varies almost twentyfold between the optimal configuration ($A \geq B$) and the less favorable configuration ($B \geq A$). Such sensitivity of the system to support stiffness distribution highlights the importance of correct placement of elastic elements in rotating machinery. In many mechanical designs, safety factors typically range from 1.5 to 3.0; therefore, geometric optimization of support elements may play a role comparable to material selection in reducing operational stresses [16].

The identified relationship between elastic element parameters and support reaction forces suggests that adjusting the stiffness of the supports may provide an effective method for controlling load distribution within the shaft system. Similar approaches have been considered in modern studies of rotor dynamics, where elastic supports are used to improve vibration stability and reduce load concentrations in rotating machinery [6], [7].

A comparison with previously published research shows that many studies describe the influence of elastic supports primarily from a qualitative perspective. However, detailed quantitative relationships between geometric parameters of elastic elements and the resulting stress distribution are rarely reported [8], [9]. The results obtained in the present work provide numerical dependencies that may be directly used in engineering calculations when designing shaft support systems with elastic elements.

Thus, the presented analysis confirms that appropriate selection of elastic element thickness can significantly influence the mechanical behavior of the shaft system and improve the operational reliability of rotating machinery.

4. Conclusions

In contrast, Model 2 ($B \geq A$) shows a significant increase in stress from 8.83×10^6 Pa to 183×10^6 Pa, which corresponds to more than a twentyfold increase. This behavior is associated with the initially low stress level at the baseline configuration and the subsequent rapid growth due to stiffness redistribution.

Reaction forces at supports correlate directly with local elastic element thickness. Support B reaction force varies by ±2.7 % (918-943 N) depending on thickness distribution, enabling predictive load management.

Optimal design recommends $A \geq B$ thickness ratio for sawing cylinder applications, achieving minimum operational stresses (112×10^6 Pa) and extended service life.

The developed computational models provide reliable tools for elastic support parameter optimization in precision shaft systems.

The results of this study can be used in the design and optimization of rotor-bearing systems with elastic supports in industrial applications.

The proposed approach contributes to improved design strategies for rotor-bearing systems with elastic supports under asymmetric stiffness conditions.

Acknowledgements

The authors have not disclosed any funding.

Data availability

The datasets generated during and/or analyzed during the current study are available from the corresponding author on reasonable request.

Conflict of interest

The authors declare that they have no conflict of interest.

References

[1] H. D. Nelson, "A finite rotating shaft element using Timoshenko beam theory," *Journal of Mechanical Design*, Vol. 102, No. 4, pp. 793–803, Oct. 1980, https://doi.org/10.1115/1.3254824

[2] D. M. Mukhammadiev, F. H. Ibragimov, and O. H. Abzoirov, "Performance analysis of a linter machine with a new design of intersaw pad," (in Russian), *Modern Innovations, Systems and Technologies*, Vol. 2, No. 3, pp. 0401–409, 2022, https://doi.org/10.47813/2782-2818-2022-2-3-0401-0409

[3] W. M. Miranda and M. T. C. Faria, "Finite element method applied to the eigenvalue analysis of flexible rotors supported by journal bearings," *Engineering*, Vol. 6, No. 3, pp. 127–137, Jan. 2014, https://doi.org/10.4236/eng.2014.63016

[4] A. Chasalevris and F. Dohnal, "Vibration quenching in a large scale rotor-bearing system using journal bearings with variable geometry," *Journal of Sound and Vibration*, Vol. 333, No. 7, pp. 2087–2099, 2014, https://doi.org/10.1016/j.jsv.2013.11.034

[5] G.-D. Wang, A.-D. Feng, C.-L. Xie, and H.-Q. Yuan, "Vibration and stability analysis of a spinning shaft with arbitrary boundaries subjected to partial load," *Journal of Vibration and Control*, Vol. 30, No. 5-6, pp. 1378–1390, 2023, https://doi.org/10.1177/10775463231163613

[6] S. Z. Yunusov, S. A. Makhmudova, D. A. Kasimova, and M. M. Agzamov, "The influence of changes in technological loads on the deflection of the saw cylinder shaft of a linting machine," *Material and Mechanical Engineering Technology*, Vol. 2025, No. 1, 2025, https://doi.org/10.52209/2706-977x_2025_1_8

[7] L. Niu, H. Cao, Z. He, and Y. Li, "A systematic study of ball passing frequencies based on dynamic modeling of rolling ball bearings with localized surface defects," *Journal of Sound and Vibration*, Vol. 357, pp. 207–232, Nov. 2015, https://doi.org/10.1016/j.jsv.2015.08.002

[8] F. Adilov, S. Makhmudova, R. Abirov, E. Toshmatov, and I. Maxmudova, "To assessment of stress-strain state in rock continua," *IOP Conference Series: Materials Science and Engineering*, Vol. 869, No. 7, p. 072019, Jun. 2020, https://doi.org/10.1088/1757-899x/869/7/072019

[9] A. Berdiev, G. Bahadirov, Z. Dong, and W. Xuelin, "Dynamic analysis of the AGV forklift," in *2022 2nd International Conference on Electronic Information Engineering and Computer Technology (EIECT)*, pp. 269–275, 2022, https://doi.org/10.1109/eiect58010.2022.00059

[10] Y. Sun et al., "Dynamic modelling of gear-rotor-bearing systems with nonlinear factors," *Mechanical Systems and Signal Processing*, 2021.

[11] A. Antonov, K. Nurmetov, A. Riskulov, V. Struk, and W. Xuemin, "Composite materials based on polyolefins modified with carbon-containing components," *Vibroengineering Procedia*, Vol. 60, pp. 458–465, Dec. 2025, https://doi.org/10.21595/vp.2025.25690

[12] M. I. Friswell, J. E. T. Penny, S. D. Garvey, and A. W. Lees, *Dynamics of Rotating Machines*. Cambridge University Press, 2010, https://doi.org/10.1017/cbo9780511780509

[13] A. Antonov, K. Nurmetov, A. Riskulov, T. Urazbaev, V. Struk, and D. Nakhvat, "Composite thermoplastic materials for filament production in 3D printing technology," *Vibroengineering Procedia*, Vol. 60, pp. 424–430, Dec. 2025, https://doi.org/10.21595/vp.2025.25691

[14] M. I. Ruzmatov, D. M. Azimov, and N. A. Korshunova, "A new class of intermediate thrust arcs in the restricted three-body problem," *Advances in Space Research*, Vol. 71, No. 1, pp. 369–374, Jan. 2023, https://doi.org/10.1016/j.asr.2022.08.063

[15] J. S. Rao, *Rotor Dynamics*. New Delhi: New Age International, 2011.

[16] S. Mamaev, A. Anna, S. Tursunov, D. Nigmatova, and T. Tursunov, "Mathematical modeling of torsional vibrations of the wheel-motor unit of mains diesel locomotive UZTE16M," *E3S Web of Conferences*, Vol. 401, p. 05014, Jul. 2023, https://doi.org/10.1051/e3sconf/202340105014

[17] G. Nan, Y. Zhang, Y. Zhu, and W. Guo, "Nonlinear dynamics of rotor system supported by bearing with waviness," *Science Progress*, Vol. 103, No. 3, pp. 1–18, Aug. 2020, https://doi.org/10.1177/0036850420944092

[18] E. Nematov, A. Berdiev, and P. Wang, "Kinematic parameters of the biplanetary mechanism (intermittent mixing machines)," *Manufacturing Technology*, Vol. 23, No. 5, pp. 685–690, 2023, https://doi.org/10.21062/mft.2023.073

[19] G. Genta, *Dynamics of rotating systems*. New York, NY: Springer US, 2005, https://doi.org/10.1007/0-387-28687-x

[20] M. Lalanne and G. Ferraris, *Rotordynamics Prediction in Engineering*. Chichester: Wiley, 1998.

[21] S. Makhmudova, N. Tursunov, and G. Avazova, "Planar dynamic modeling of a rotor-bearing-housing system with polyurethane support layer," *Vibroengineering Procedia*, Vol. 60, pp. 1–7, Dec. 2025, https://doi.org/10.21595/vp.2025.25509